Available online at www.sciencedirect.com
SCIENCE DIRECT®
Chemical Physics Letters 408 (2005) 145–149
CHEMICAL PHYSICS LETTERS
www.elsevier.com/locate/cplett

Theoretical interpretation of different nanotube morphologies among Group III (B, Al, Ga) nitrides

Min Zhang [a], Zhong-Min Su [a,*], Li-Kai Yan [a], Yong-Qing Qiu [a], Guan-Hua Chen [b,*], Rong-Shun Wang [a]

[a] *Institute of Functional Material Chemistry, Faculty of Chemistry, Northeast Normal University, No. 5268 Renmin Street, Changchun, Jinlin 130024, China*
[b] *Department of Chemistry, The University of Hong Kong, Pokfulam Road, Hong Kong, China*

Received 9 December 2004; in final form 5 April 2005
Available online 4 May 2005

Abstract

Three different nanotube structures, armchair, zigzag and wurtzite, were studied using B3LYP/6-31G(d) for carbon, BN, AlN and GaN nanotubes, respectively. Our calculations found that AlN and GaN can implausibly form the usual tubular morphologies of carbon and BN nanotubes. The same conclusion was confirmed based on analyzing the different configurations of benzene, borazine, and the analogies of the hexagonal $Al_3N_3H_6$ and $Ga_3N_3H_6$ at the same level of calculations.

1. Introduction

Nanotubes have been a focus of researches and received increasing attention during the past 10 years, due to their unique and fascinating properties, and wide potential applications. After the discovery of carbon nanotubes in 1991 [1], the nanotubes composed of other chemical compositions have also been investigated [2,3]. Among them, the binary materials composed of Group III nitrides [4,5] are viewed as ideal analogs of carbon because of their isoelectrons in hexagon network and potential use in light emittance device [6,7]. BN is the first candidate to replace carbon, because hexagonal-BN structure ($a = 2.50$ Å, $c = 6.66$ Å) is quite similar to that of graphite ($a = 2.46$ Å, $c = 6.71$ Å). The successful synthesis of pure BN nanotubes was reported in 1995 [8]. BN nanotubes are also divided into armchair, chiral and zigzag structures. Theoretical studies predicted that BN nanotubes are dominant in zigzag arrangement and are wide band gap semiconductors with a band gap of 5.5 eV [9,10], independent on the tube diameter and the chirality. These properties were subsequently ascertained by the experimental results. Other properties of the BN nanotubes were also investigated theoretically [11–14]. Owing to the great success of BN nanotubes, the structural stability and electronic properties of AlN [15–17] and GaN [18] nanotubes with the conventional carbon nanotubes morphologies were investigated. Recently, GaN nanotubes were synthesized by an 'epitaxial casting' approach by Yang and co-workers [19]. The GaN nanotubes with lengths of ca. 2–5 μm, diameters of 30–200 nm, and the wall thicknesses of 5–50 nm, were reported. Soon after, the AlN nanotubes were synthesized by Hu and co-workers [20] (in a horizontal tubular furnace). The nanotubes were reported to be several micrometers in length with the diameters from 30 to 80 nm. Surprisely, the results of electron diffraction and X-ray diffraction (XRD) measurements showed that the morphologies of those obtained AlN and GaN nanotubes are differed from the conventional

* Corresponding authors. Fax: +86 431 5684009 (Z.-M. Su).
E-mail addresses: zmsu@nenu.edu.cn (Z.-M. Su), ghc@yangtze.hku.hk (G.-H. Chen).

0009-2614/$ - see front matter © 2005 Elsevier B.V. All rights reserved.
doi:10.1016/j.cplett.2005.04.025

carbon nanotubes, and they are the wurtzite structure which orientates along their c axis was observed.

The apparent distinction of the morphology among carbon, BN, AlN and GaN nanotubes calls for further theoretical investigations. The aim of this Letter is to provide a theoretical exploration in the discrepant morphology: i.e., why AlN and GaN can not form the conventional morphologies similar to carbon and BN nanotubes.

2. Models and computational methods

The single-walled carbon nanotube can be viewed as infinite graphite rolled up to form a tube. The chiral vector C_h and the helicity θ are introduced during the curling. A nanotube is defined by the chiral vector C_h, given by equation: $\vec{C}_h = n\vec{a}_1 + m\vec{a}_2$, where the integers n and m are the numbers of steps along the two unit vectors of the hexagonal lattice, $\vec{a}_1$ and $\vec{a}_2$, respectively. The vector C_h connects two crystallographically equivalent sites and the chiral angle θ is the angle which makes with respect to the zigzag direction. There exist two limiting cases that the chiral angles are 0° and 30°. They are referred to zigzag nanotube (0°) and armchair nanotube (30°), which are two important structures of carbon nanotubes.

Three different structures, armchair (as shown in Fig. 1a), zigzag (Fig. 1b) and wurtzite orientated along their c axis (Fig. 1d), were constructed and investigated for carbon, BN, AlN and GaN nanotubes, respectively. The (3,3) armchair (5,0) zigzag nanotubes and the small wurtzite structure were used in the calculations to save the computation time [21,22]. The properties of these inorganic nantobes were also obtained from these simplified models [3,15]. Both ends of these systems are terminated with hydrogen atoms. It should be announced that these systems may be not electronically stable as their crystal species, however they are useful to understand the electronic and bonding properties in nanophase [15,21,22].

The DFT B3LYP calculations on these systems were carried out. Geometry optimization was also performed with standard polarized 6-31G(d) basis set. Harmonic frequency analysis at the same level was used to examine the stability of those optimized structures, and to evaluate zero-point energy (ZPE). The calculations were run with the GAUSSIAN 98 program suite [23].

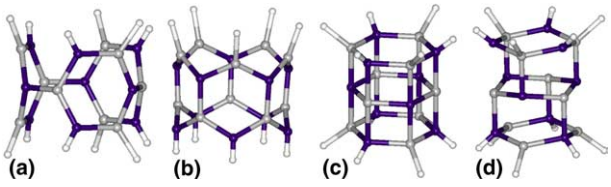

Fig. 1. (a) (3,3) Armchair structure. (b) (5,0) Zigzag structure. (c) hexagonal structure. (d) Wurtzite structure. For carbon nanotube (○, ● = C) and for other nanotubes (○ = N, ● = B, Al, Ga).

3. Results and discussion

It is very interesting to note that all the wurtzite structures finally turn into hexagonal structures (as shown in Fig. 1c) after structural optimization. The reason is mainly originated from the small diameter of the calculated systems for a stable wurtzite structure. However, such analysis is significant and valuable to explore the difference of morphology among carbon, BN, AlN, and GaN nanotubes.

These calculated results of carbon and BN structures listed in Table 1 reveal that the total energies of all those three structures (as seen as a–c in Fig. 1) are local minima. The hexagonal structures in AlN and GaN systems are the most stable. The identical stoichiometry of hexagonal and armchair structures of those four systems allows us to compare their total energies directly. The results indicate that the hexagonal structures are less stable than the armchair in carbon and BN systems. To further validate this conclusion, the calculation is also carried out on the nanotubes with two repeat units, and the same conclusion is obtained finally.

For carbon hexagonal structure, lengths of the C–C bond for the intrahexagonal and interlayer bonds are 1.566 and 1.583 Å, respectively. For BN hexagonal structure, the intrahexagonal bond length is 1.581 Å, and the interlayer bond length is 1.611 Å. These bonds belong to a non-classical tetrahedral topological structure (sp^3 hybridization). This high stability of these compounds is derived much from the π_σ–π_σ orbital interaction between the parallel rings, as illustrated recently by Hoffmann and co-workers [24].

Table 1
Computed total energies with ZPE correction (unit: a.u.), and the number of imaginary frequencies (N_{imag})

Morphology	E^T with ZPE correction (a.u.)			N_{imag}		
	a	*b*	*c*	*a*	*b*	*c*
C						
(1 unit)	−692.668	−767.520	−692.212	0	0	0
(2 unit)	−1149.795	−1148.414	−1148.639	0	0	0
BN						
(1 unit)	−724.149	−802.635	−723.803	0	0	0
(2 unit)	−1202.356	−1201.121	−1201.441	0	0	0
AlN						
(1 unit)	−2682.468	−2978.562	−2682.626	1	2	0
(2 unit)[a]	−4442.978	−4465.018	−4443.211	2	2	0
GaN						
(1 unit)	−17806.705	−19783.265	−17806.891	5	2	0
(2 unit)[a]	−29559.844	−29558.681	−29560.022	2	1	0

[a] Calculated with B3LYP/3-21G*.

The situation is quite different for the case of AlN and GaN nanotubes. The energies of the hexagonal structures are lower than those of the armchair nanotubes (data shown in Table 1). More importantly, the armchair and zigzag structures are unstable due to those imaginary frequencies in our calculations. It gives a clear explanation why the armchair and zigzag nanotubes of AlN and GaN are not observed in the experiments. The bond lengths of the hexagonal structures (listed in Fig. 2a) are almost the same with their crystal counterparts. The difference between the theoretical length of interlayer bond and practical structure is only 0.009 Å for AlN, and 0.012 Å for GaN. It is well known that the chemical bonds in the hexagonal structures belong to the non-classical tetrahedral topology, as mentioned earlier [24]. The same conclusion can also be found in AlN and GaN systems with two unit length.

To further study the stability of sp^2 hybridized AlN and GaN nanotubes, HOMO distributions of BN and GaN armchair nanotubes are shown in Fig. 3. The same isodensity value, 0.015, was employed for both HOMO orbitals. An obvious distinction between their two HOMOs can be seen in Fig. 3. The p_z electrons are delocalizing on the whole BN nanotube. The delocalization on GaN is much weaker than that on BN. All these results strongly suggest that sp^2 hybridization is much unstable in Al and Ga nitrides.

We may understand the nature of bonding in all these structures from another point of view. Carbon nanotubes are composed of bending benzenes (π-conjugated six-membered rings), which are linked each other. For example, (3,3) armchair nanotube of one unit consists of three bending benzenes linked together by C–C

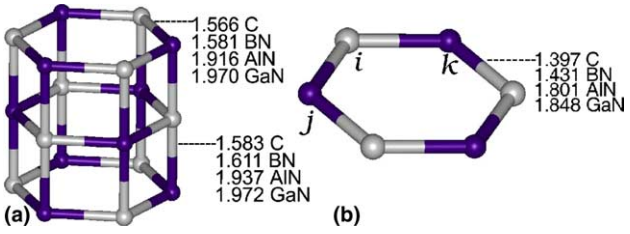

Fig. 2. Optimized bond lengths (Angstrom) of hexagonal structures (a), and π-conjugated six-membered rings (b), H hidden.

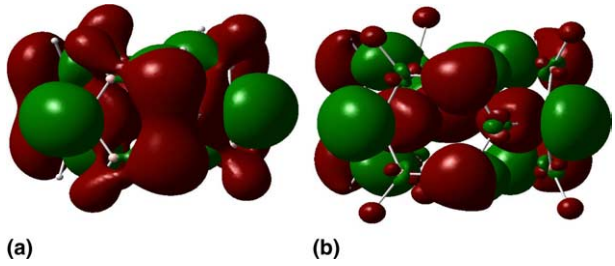

Fig. 3. Isodensity surfaces of the HOMO distributions (3,3) armchair nanotubes: (a) for BN; (b) for GaN.

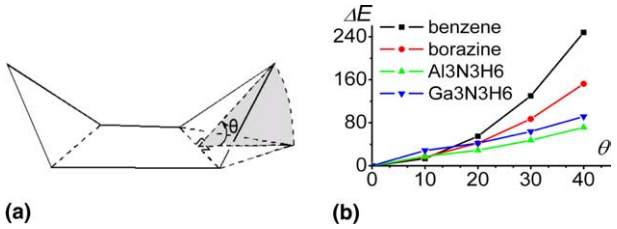

Fig. 4. Schematic diagram for structure folding (a), and elastic strain energies with ZPE (kJ mol^{-1}) vs. θ (b).

bonds. The folding angle θ (shown in Fig. 4a) varies inversely as the diameter of nanotube. For (3,3) armchair nanotube, θ is ca. 30°. It is very useful to analyze the configuration energies at different θs in order to understand the possibility and the consumed energy for carbon, BN, AlN and GaN to turn them into the usual carbon nanotube morphology.

First, the structures of benzene, borazine, and hexagonal $Al_3N_3H_6$ and $Ga_3N_3H_6$ (bond lengths shown in Fig. 2b) was determined using the same B3LYP/6-31G(d) calculation. All the atoms are in the same plane with the π-conjugated skeleton for $Al_3N_3H_6$ and $Ga_3N_3H_6$. Harmonic frequency analysis shows all of them to be minima and stable. The calculated total C–C bonding dissociation energy (BDE) in benzene is 636.5 kJ mol^{-1}, which is very close to the experiment value 614 kJ mol^{-1}. The B–N total BDE is 602.8 kJ mol^{-1}, a little lower than that of C–C bond. However, the BDEs of Al–N and Ga–N are only 517.3 and 422.6 kJ mol^{-1}, respectively. The standard scaling factor 0.9614 for B3LYP/6-31G(d) is used for vibrational frequencies [25]. The scaled stretching vibrational frequencies of benzene and borazine are 1592.4 and 1435.7 cm^{-1}, respectively, and both are consistent to the experimental values at 1600 and 1420 cm^{-1} [26]. However, the Al–N and Ga–N scaled stretching frequencies are only 847.0 and 777.8 cm^{-1}, respectively. These indicates that the delocalized π bond in the systems of Al–N and Ga–N are much weaker than those of B–N and C–C.

Furthermore, the natural bond order is also calculated with natural resonance theory employing 6-31G(d) basis set [27]. The effective atomic configuration of each non-hydrogen atoms takes the idealized sp^2 hybridization, according to the natural population analysis. It can be seen clearly from Table 2 that C–C bonds

Table 2
The calculated bond order with natural resonance theory for benzene analogues (*i*, *j*, *k* shown in Fig. 2b)

	i–j			*i–k*		
	Total	Covalent	Ionic	Total	Covalent	Ionic
Benzene	1.4845	1.4663	0.0182	1.4845	1.4663	0.0182
Borazine	1.8052	0.6547	1.1505	1.0843	0.4741	0.6102
$Al_3N_3H_6$	1.8626	0.3551	1.5075	1.0330	0.2442	0.7888
$Ga_3N_3H_6$	1.8443	0.4216	1.4227	1.0283	0.3040	0.7243

are well delocalized in benzene, and are almost entirely covalent bonding. It is well known that the π electron delocalization in borazine may be expected to be reduced as compared to benzene, and the ionicity is more than 50%, because of the large electronegativity difference between boron (2.0) and nitrogen (3.0). And all the B–N bonds in borazine have almost the same length and bonding energy suggesting it as 'inorganic benzene'. The systems of $Al_3N_3H_6$ and $Ga_3N_3H_6$ show more ionicity and less covalence. Moreover, their bonding energies are decreasing with the increase of their bond lengths. It indicates that the sp^2 hybridization in $Al_3N_3H_6$ and $Ga_3N_3H_6$ sounds reasonable, but quite unstable. The reason is mainly assigned to quite small overlap between the outer p_z orbital of Al or Ga and the N p_z orbital, which may originate from the larger difference in the atomic radii and in electronegativities. This leads to much weaker π bondings of Al–N and Ga–N in comparison with the case of B–N and carbon.

Their bending energies were calculated too, and the reasonable bending configurations were examined by counting the number of imaginary frequencies. Then, the natural populations and the natural bond orders were recalculated at corresponding angle with the same level. Their sp^2 hybridization and their bond components are consistent with the original planar configuration. It can be seen from Fig. 4 that the elastic strain energy of borazine is smaller than that of benzene at the same θ. The same result, as obtained by Blaxe et al. [9], can be concluded that BN nanotubes are energetically more favorable than carbon nanotubes. The elastic strain energies of $Al_3N_3H_6$ and $Ga_3N_3H_6$ are much less than those of benzene and borazine at the same θ. The less elastic energy of Group III nitrides should be derived from their high ionic bond components, because ionic bond is non-directional, whereas covalent bond is directional. These results are also consistent with the calculations for AlN [16,17] and GaN [18]. The lowest vibrational frequencies at different θs are listed in Table 3, for revealing the bending effect on the stability. However, the lowest frequencies of AlN and GaN decrease dramatically with increases of θ. No imaginary frequency at a higher θ (larger than 40°) can be found for benzene and borazine. It suggests that the nanotubes composed of bending benzene and borazine is stable and practical. The imaginary frequencies for $Al_3N_3H_6$ is obtained at 30°, and for $Ga_3N_3H_6$ is at 10°. It indicates that the nanotubes morphologies based on the bending $Al_3N_3H_6$ and $Ga_3N_3H_6$ are impossible in nature. This also suggests that the instability of AlN and GaN nanotubes with the conventional carbon nanotubes morphologies is not originated from the large elastic energies, as suggested early [20], actually it should be from the unfavorable non-planar sp^2 hybridization.

Table 3
Computed the lowest scaled vibration frequency at different bending angle θ unit: (cm^{-1})

θ	0	10	20	30	40
Benzene	398.9	398.2	396.8	393.2	385.3
Borazine	277.9	233.1	228.4	210.9	126.8
$Al_3N_3H_6$	129.7	34.6	23.9	−45.5	−97.4
$Ga_3N_3H_6$	132.5	−40.2	−77.7	−99.1	−120.4

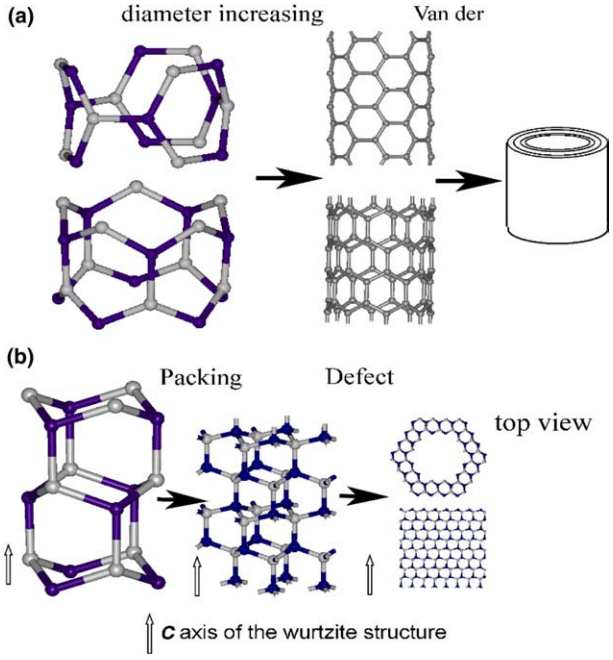

Fig. 5. Scheme for the different nanotube morphologies: (a) for C and BN; (b) for AlN and GaN.

The different nanotube morphologies among C, BN, AlN and GaN are illustrated in Fig. 5. The carbon and BN nanotubes are formed as a graphite structure based on the sp^2 hybridization. The nanotube diameter ranges widely from less than one nanometer to hundreds of nanometer. The interaction between layers of multiwalled nanotubes is van der Waals force (seen in Fig. 5a). However, it is impossible for AlN and GaN to form similar carbon nanotube morphologies based on sp^2 hybridization. The chemical bonding in AlN and GaN nanotubes must be dependent on the fourfold coordination (diamond-like structure). The wurtzite crystal nanowires can form a unit-cell packing alone c axis. Such nanotubes are part of the defect structure in the center of the nanowires (shown in Fig. 5b), which can be obtained commonly using *epitaxial casting* [19] and *growing in a horizontal tubular furnace* [20].

4. Summary

Our calculations confirmed that it is implausible for AlN and GaN to form the tubular morphologies of

carbon and BN. The reason is from the weaker overlap between Al's (Ga's) and N's p_z orbitals. The calculations also verified that the bending benzene analogues (π-conjugated six-membered rings) are very useful models in exploring the stability of the nanotube morphology based on sp^2 hybridization.

Acknowledgments

Authors acknowledged financial supports from the National Natural Science Foundation of China (Nos. 20373009 and 20162005) and the Youth Fund of Northeast Normal University (No. 111494019). The support from the Fund of State Key Laboratory of Theoretical and Computational Chemistry, Jilin University, is also gratefully acknowledged.

References

[1] S. Iijima, Nature 354 (1991) 56.
[2] C.N.R. Rao, M. Nath, Dalton Trans. 1 (2003) 1.
[3] M. Zhang, Y.H. Kan, Q.J. Zang, Z.M. Su, R.S. Wang, Chem. Phys. Lett. 379 (2003) 81.
[4] J. Hu, Y. Bando, D. Golberg, Q. Liu, Angew. Chem., Int. Ed. 42 (2003) 3493.
[5] M. He, I. Minus, P. Zhou, N. Mohammed, J.B. Halpern, Appl. Phys. Lett. 77 (2003) 3731.
[6] V. Meunier, C. Roland, J. Bernholc, Appl. Phys. Lett. 81 (2002) 46.
[7] V.N. Tondare, C. Balasubramanian, S.V. Shende, D.S. Joag, V.P. Godbole, Appl. Phys. Lett. 80 (2002) 4813.
[8] N.G. Chopra, R.J. Luyken, K. Cherrey, V.H. Crespi, M.L. Cohen, S.G. Louie, A. Zettl, Science 269 (1995) 966.
[9] X. Blaxe, A. Rubio, S.G. Louie, M.L. Cohen, Europhys. Lett. 28 (1994) 335.
[10] H.Y. Zhu, D.J. Klein, W.A. Seitz, N.H. March, Inorg. Chem. 34 (1995) 1377.
[11] T.M. Schmidt, R.J. Baierle, P. Piquini, A. Fazzio, Phys. Rev. B 67 (2003) 113407.
[12] F.F. Xu, Y. Bando, D. Golberg, R.Z. Ma, Y.B. Li, C.C. Tang, J. Chem. Phys. 119 (2003) 3436.
[13] B. Akdim, R. Pachter, X. Duan, W.W. Adarms, Phys. Rev. B 67 (2003) 245404.
[14] H.Y. Zhu, D.J. Klein, N.H. March, A. Rubio, J. Phys. Chem. Solids 59 (1998) 1303.
[15] D. Zhang, R.Q. Zhang, Chem. Phys. Lett. 371 (2003) 426.
[16] M.W. Zhao, Y.Y. Xia, D.J. Zhang, L.M. Mei, Phys. Rev. B 68 (2003) 235415.
[17] M.W. Zhao, Y.Y. Xia, Z.Y. Tan, X.D. Liu, F. Li, B.D. Huang, Y.J. Ji, L.M. Mei, Chem. Phys. Lett. 389 (2004) 160.
[18] S. Lee, Y.H. Lee, Y.G. Hwang, J. Elsner, T. Frauenheim, Phys. Rev. B 60 (1999) 7788.
[19] J. Goldberger, R. He, Y. Zhang, S. Lee, H. Yan, H.J. Choi, P.D. Yang, Nature 422 (2003) 599.
[20] Q. Wu, Z. Hu, X. Wang, Y. Lu, X. Chen, H. Xu, Y. Chen, J. Am. Chem. Soc. 125 (2003) 10177.
[21] W.Z. Liang, S. Yokojima, M.F. Ng, G.H. Chen, G. He, J. Am. Chem. Soc. 123 (2001) 9830.
[22] W.Z. Liang, G.H. Chen, Z.M. Li, Z.K. Tang, Appl. Phys. Lett. 80 (2002) 3415.
[23] M.J. Frisch et al., GAUSSIAN 98, Gaussian, Inc., Pittsburgh, PA, 2001.
[24] R.M. Minyaev, V.I. Minkin, T.N. Gribanova, A.G. Starikov, R. Hoffmann, J. Org. Chem. 68 (2003) 8588.
[25] J.B. Foresman, A. Frisch, Exploring Chemistry with Electronic Structure Method, Gaussian, Inc., Pittsburgh, PA, 1996.
[26] J.B. Lambert, H.F. Shurvell, D.A. Lightner, R.G. Cooks, Organic Structural Spectroscopy, Prentice Hall, Englewood Cliffs, NJ, 1998.
[27] S.F. Feldgus, C.R. Landis, E.D. Glendening, et al., J. Comput. Chem. 21 (2000) 411.